J Mol Model (2013) 19:1617–1626
DOI 10.1007/s00894-012-1724-5

ORIGINAL PAPER

Theoretical studies on the unimolecular decomposition of nitroglycerin

Qingli Yan · Weihua Zhu · Aimin Pang · Xuhui Chi · Xijuan Du · Heming Xiao

Received: 14 November 2012 / Accepted: 3 December 2012 / Published online: 3 January 2013

Abstract To improve the understanding of the unimolecular decomposition mechanism of nitroglycerin (NG) in the gas phase, density functional theory calculations were performed to determine various decomposition channels at the B3LYP/6-311G** level. For the unimolecular decomposition mechanism of NG, we find two main mechanisms: (I) homolytic cleavage of O-NO_2 to form •NO_2 and $CH_2ONO_2CHONO_2CH_2O$•, which subsequently decomposes to form •CHO, •NO_2, and $2CH_2O$; (II) successive HONO eliminations to form HONO and CHO-CO-CHO, which subsequently decomposes to form CH_2O+2CO_2 and •CHO+CO. We also find that the former channel has slightly smaller activation energy than the latter one. In addition, the rate constants of the initial process of the two decomposition channels were calculated. The results show that the O-NO_2 cleavage pathway occurs more easily than the HONO elimination.

Keywords Density functional theory · Homolytic cleavage · HONO elimination · Nitroglycerin · Rate constants · Transition state

Introduction

Nitroglycerin (NG) is not only one kind of liquid nitrate ester explosive but also a major energetic plasticizer in nitrate ester plasticized polyether (NEPE) propellants and other double-based propellants [1–8]. NG in the propellant formulations tends to decompose with time, releasing nitrogen oxides as the most reactive part of the whole decomposition products. The nitrogen oxides accelerate the degradation of nitrate ester by autocatalysis and so shorten the service lifetime of the NEPE propellants. In addition, the decomposition of NG is related closely with the combustion and thermal stability of the NEPE propellants. Therefore, the knowledge of the thermal decomposition of NG is very useful for understanding the aging phenomena and determining the rules of the combustion and thermal stability of the NEPE propellants.

Until now, there are a large number of studies devoted to the decomposition of NG [1, 3, 9–13]. As early as 1970, Waring and Krastins [9] investigated the thermal decomposition of NG in the vapor and liquid phases and proposed a mechanism for the vapor-phase reaction. Sadasivan and Bhaumik [1] indicated that the initial step in the decomposition of doubled-based propellant is the O-NO_2 breaking of NG and NC (nitrocellulose). Roos and Brill [10] proposed that the decomposition products of NG are CO_2, CO, NO_2, NO, HNCO, O_2, H_2O, CH_2O, H_2, N_2, and N_2O at 400 °C and the pressure of 5 MPa and the major products are NO_2 and CH_2O. Hiyoshi and Brill [11] employed T-Jump/FTIR spectroscopy to flash pyrolyze NG and found that the decomposition products of NG at 350 °C and the pressure of 0.5 MPa are CO_2, CO, NO_2, NO, HCN, HONO, H_2O, CH_2O, H_2, and N_2. Chin et al. [12] mentioned that the initiation step of the decomposition of NG and NC is the rupture of the O-NO_2 bond. By isothermal thermogravimetry experiments, Sućeska et al. [14, 15] found that at a very early stage the evaporation of NG from a double base rocket propellant can be described by the zero-order reaction model, in line with the results obtained by Tompa et al. [14, 15].

In addition, many other alkyl nitrate esters have widely investigated [9, 12, 16–22]. These studies indicate that the initial decomposition process of alkyl nitrate esters is the rupture of the O-NO_2. The product RCH_2O• is an important intermediate, which has many patterns of transformation

Q. Yan · W. Zhu (✉) · H. Xiao
Institute for Computation in Molecular and Materials Science and Department of Chemistry, Nanjing University of Science and Technology, Nanjing 210094, China
e-mail: zhuwh@njust.edu.cn

A. Pang · X. Chi · X. Du
Hubai Institute of Aerospace Chemotechnology, Xiangyang 441003, China

such as single molecule cracking, isomerization, and H-migration. Since NG is an important alkyl nitrate ester, the information will be useful to improve the understanding of the decomposition mechanism of NG.

Very few theoretical studies on the decomposition of NG have previously been reported. However, the theoretical studies on other nitrate esters have been reported [23–28]. Earlier theoretical studies on cellulose and NC show that the O-NO_2 bond is the weakest bonds and the initial step in the decomposition is the O-NO_2 breaking [29]. The molecular structures, vibrational spectra, standard thermodynamic functions, and heats of formation of seven nitric esters including NG were calculated at the HF, B3LYP, and MP2 levels with the 6-31G* basis set [24]. Li et al. suggested that the O-NO_2 bond was a trigger bond during thermal decomposition process for nitric esters. The O-NO_2 bond dissociation energy in NG is also calculated to be 142.04 kJ mol^{-1} at the B3LYP/6-31G* level [27].

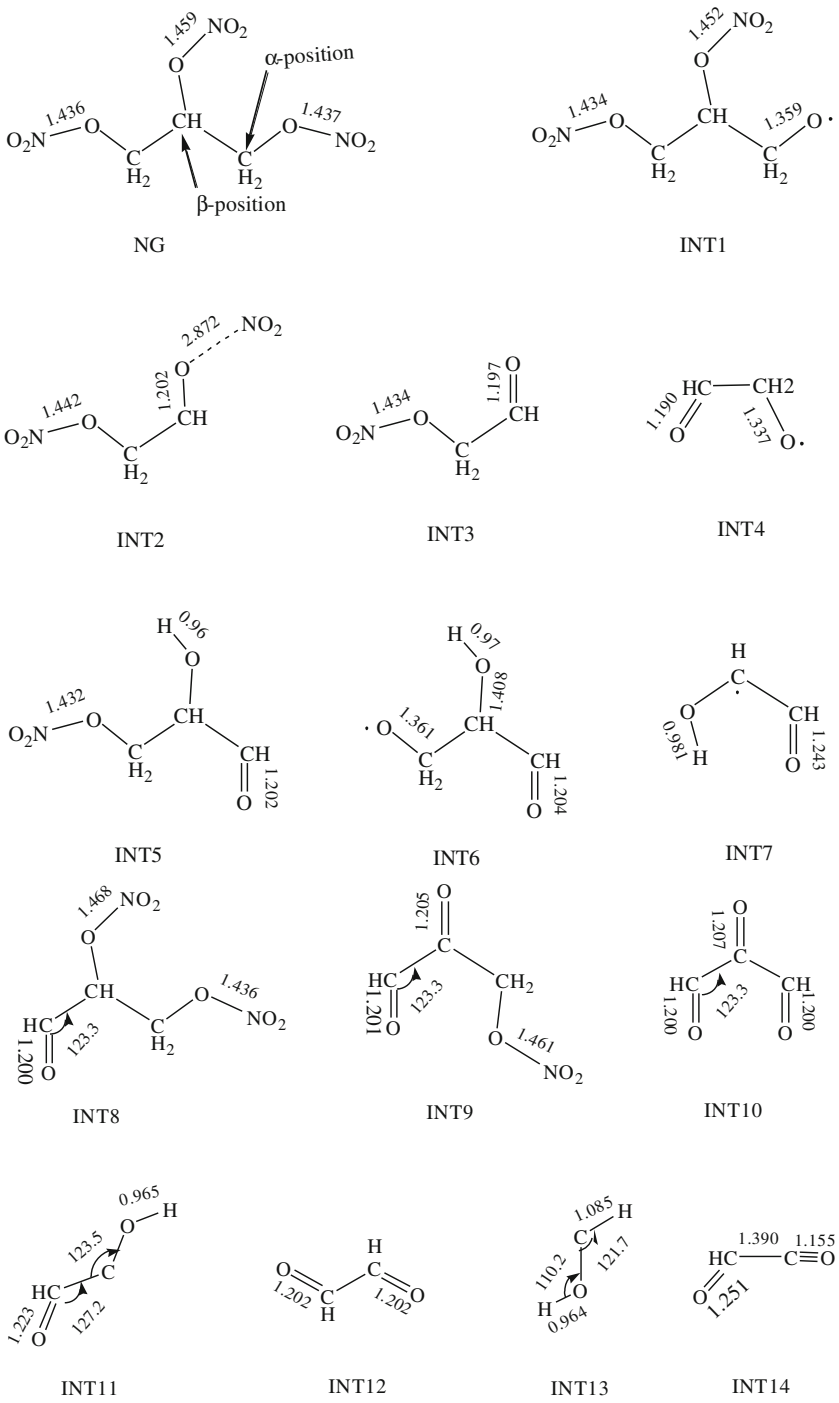

Fig. 1 Optimized structures of NG and the intermediates in the unimolecular decomposition of NG

In spite of a large number of experimental and theoretical studies on NG and other nitrate esters the decomposition mechanism of NG is still not clear enough because of the complexity and rapidness of the thermal decomposition process of NG. We only know that its initiation step of the decomposition is the breakage of O-NO_2. However, the next steps in the process are not clear.

In this work, we performed density functional theory (DFT) calculations to determine various unimolecular decomposition channels of NG at the B3LYP6-311G** level. A new different decomposition pathway of NG is found in our research and a detailed mechanism for thermal decomposition of NG is also proposed.

The remainder of this paper is organized as follows. First a brief description of our computational method is given, then the results and discussion are presented, followed by a summary of our conclusions.

Computational methods

The Becke's three parameter exchange functional and Lee-Yang-Parr (LYP) functional (B3LYP) of DFT [30, 31] is not only able to give reliable geometries, energies, and infrared vibrational frequencies but also needs less time and computer resources, which have been widely applied and have played an important role to deal with complex electron correlation problems. The molecular structures of the reactants, transition states (TS), intermediates, and products were optimized at

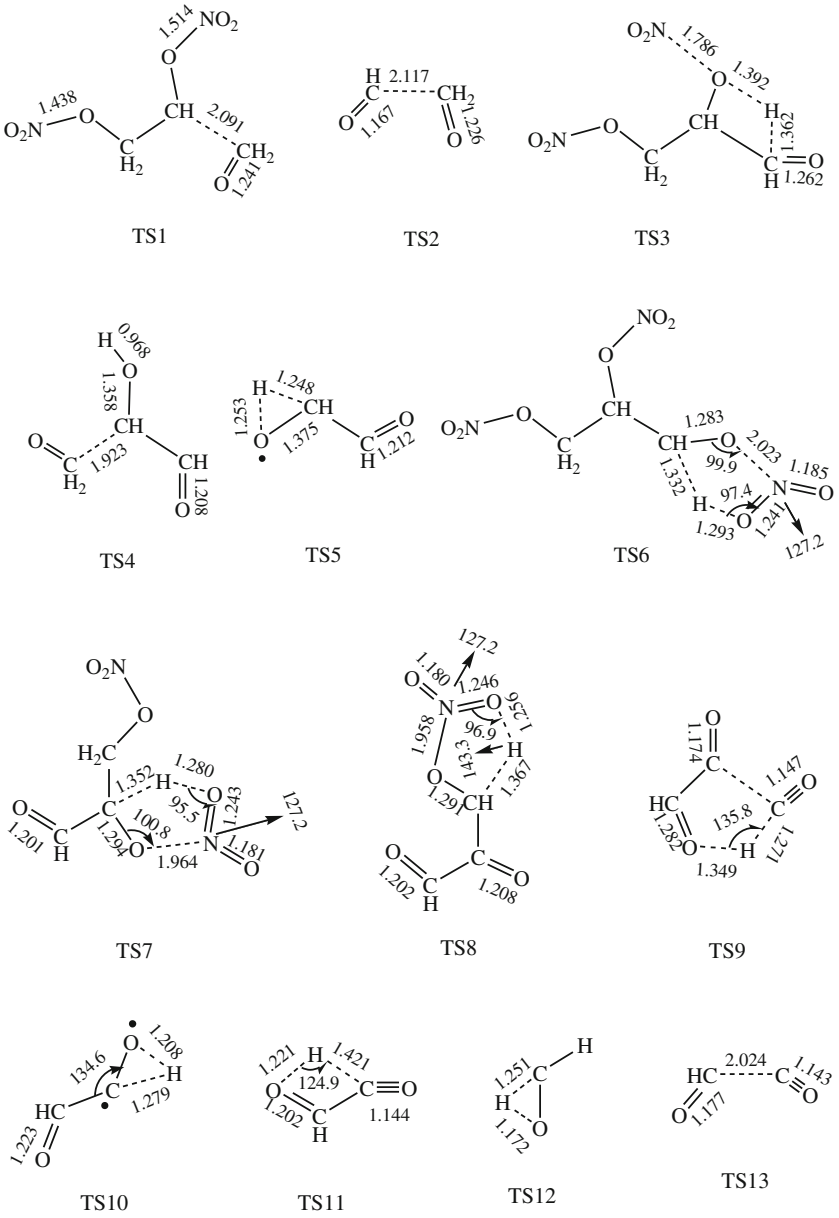

Fig. 2 Optimized structures of the transition states in the unimolecular decomposition of NG

the (U)B3LYP/6-311G** basis set and single point energies were calculated at the same level.

The corresponding vibration frequencies were also calculated at the same level to characterize a local minimum or transition state. There is only one imaginary frequency for the transition states. The transition state connected between designated reactants and products have been further verified by performing intrinsic reaction coordinate (IRC) calculations [32, 33]. All of the calculations were carried out with Gaussian 03 package of programs [34].

Results and discussion

Figure 1 displays the fully optimized geometries of NG and the intermediates, while the molecular structures of the various transition states (TS) are listed in Fig. 2. The potential energy profiles for O-NO_2 homolysis and its consequent decompositions and HONO elimination from NG and its consequent decompositions are illustrated in Figs. 3 and 4, respectively. Figure 5 presents the rate constants of two reaction channels: O-NO_2 cleavage and HONO elimination.

Tables 1 and 2 show the vibrational frequencies of the intermediates and transition states. Table 3 lists the relative energy of two possible initial steps of the decomposition: the homolytic cleavage of O-NO_2 and the HONO elimination. The energies here and in the following discussion are corrected for zero-point energy (ZPE).

Initial decomposition step and chemical equations in the two main mechanisms

There are two different orientations of NO_2 groups in the NG molecular structure as shown in Fig. 1: α-O-NO_2 and β-O-NO_2. So in which position the homolysis of O-NO_2 will occur must be considered. In addition to the dissociation of the O-NO_2 bond, there will be a competitive HONO elimination of one NO_2 group from NG. Similarly, there are two H transfers in the HONO elimination: α-H and β-H transfer. Therefore, we first investigate different possibilities for two competitive initial decomposition pathways of NG.

Table 3 lists the relative energies of the possible trigger reactions in detail. The bond dissociation energy (BDE) required for the leaving of α-NO_2 is 133.34 kJ mol^{-1}, while that required for the removal of β-NO_2 is 138.78 kJ mol^{-1}. Thus, it is apparent that the homolytic cleavage of α-O-NO_2 is preferred in the decomposition of NG. For HONO elimination, as shown in Table 3, the activation energies of the two possible elimination pathways are 143.74 and 156.72 kJ mol^{-1}, respectively. This shows that the α-H transfer will preferentially occur in the HONO elimination. The same conclusion are also obtained when we calculate at the B3LYP/6-311++G** level, as shown in Table 3.

The chemical reactions for the unimolecular decomposition mechanism of NG are listed as follows. For the homolytic cleavage of α-O-NO_2 pathway, the explicit chemical equations are:

$$\underset{\text{NG}}{CH_2ONO_2CHONO_2CH_2ONO_2} \xrightarrow{\alpha-O-NO_2\ \text{cleavage}} \underset{\text{INT1}}{CH_2ONO_2CHONO_2CH_2O\bullet} + \bullet NO_2 \quad (1)$$

$$\underset{\text{INT1}}{CH_2ONO_2CHONO_2CH_2O\cdot} \begin{cases} \xrightarrow{TS1} CH_2ONO_2\dot{C}HONO_2 + HCHO \\ \qquad\qquad \underset{\text{INT2}}{} \\ \xrightarrow{TS3} CH_2ONO_2CHOHCHO + \cdot NO_2 \\ \qquad\qquad \underset{\text{INT5}}{} \end{cases} \quad (2,3)$$

$$\underset{\text{INT2}}{CH_2ONO_2\dot{C}HONO_2} \rightarrow \underset{\text{INT3}}{\bullet OCH_2CHO} + \bullet NO_2 \quad (4)$$

$$\underset{\text{INT3}}{CH_2ONO_2CHO} \rightarrow \underset{\text{INT4}}{\bullet OCH_2CHO} + \bullet NO_2 \quad (5)$$

$$\underset{\text{INT4}}{\bullet OCH_2CHO} \xrightarrow{TS2} \bullet CHO + HCHO \quad (6)$$

$$\underset{\text{INT5}}{CH_2ONO_2CHOHCHO} \longrightarrow \underset{\text{INT6}}{\bullet OCH_2CHOHCHO} + \bullet NO_2 \quad (7)$$

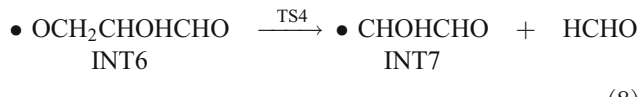

(8)

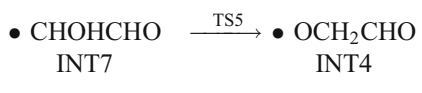

(9)

For the HONO elimination pathway by the α-H transfer, the chemical equations are:

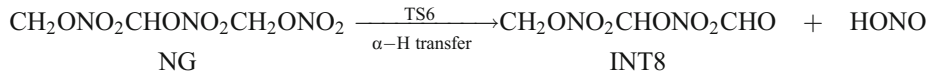

(10)

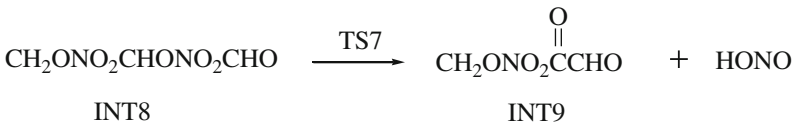

(11)

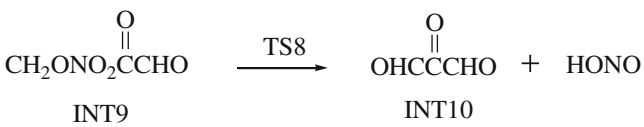

(12)

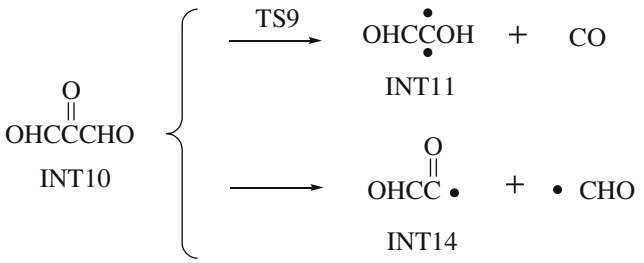

(13, 14)

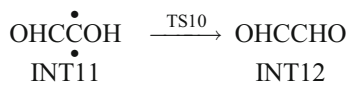

(15)

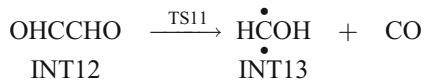

(16)

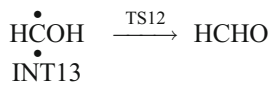

(17)

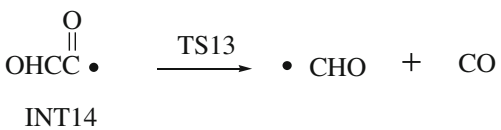

(18)

Homolytic cleavage of α-O-NO_2 plus subsequent decomposition

A number of studies [1, 9, 12, 16–22] have shown that the decomposition reactions of nitric acid ester compounds generally begin with the rupture of O-NO_2. As discussed above, the BDE of α-O-NO_2 is 133.34 kJ mol^{-1}, which is in the experimental range 107.86–209.20 kJ mol^{-1} [9, 35]. And the bond dissociation energy of O-NO_2 in NG is calculated to be 142.04 kJ mol^{-1} at the DFT-B3LYP/6-31G* level [27], which is close to our calculated value here. These comparisons confirm that our computational results are reasonably satisfactory. Among possible initial decompositions, as shown in Eq. (1), the α-O-NO_2 bond of NG may homolytically break to form INT1, and the structure of INT1 is displayed in Fig. 1. INT1 will further decompose. Equations (2) and (3) show that there may exist two possible decomposition pathways of INT1: (I) the rupture of C-C bond to form CH_2O and INT2 and (II) further cleavage of O-NO_2. Since it is difficult to determine which bond breaks first, we examined the two possible pathways as follows.

C-C bond cleavage in INT1 based on Eqs. (2), (4), (5), and (6)

INT1 is an important intermediate and its C-C bond adjacent to the radical center can break to form a single molecular CH_2O and stable INT2 via TS1. This requires an additional energy of 39.52 kJ mol^{-1}. The breaking C-C bond in TS1 is 2.091 Å. The energy of TS1+NO2 is 172.86 kJ mol^{-1} relative to NG, while INT2+CH_2O+NO_2 is 22.38 kJ mol^{-1} less than NG. Thus, the decomposition of NG to INT2+CH_2O+NO_2 is exothermic (energy released). This indicates that INT2+CH_2O+NO_2 is more stable than NG.

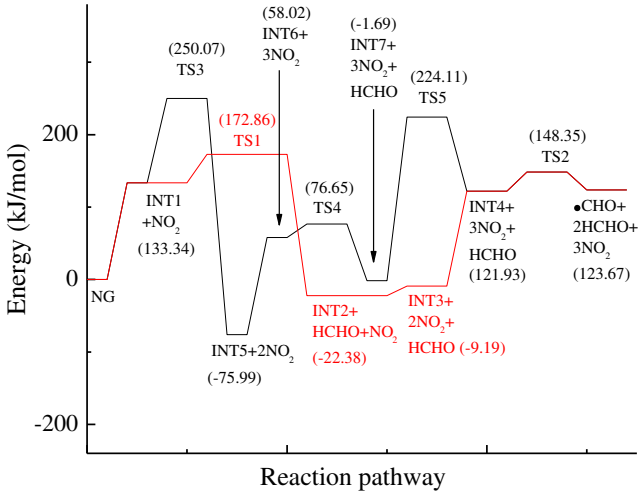

Fig. 3 Potential energy profiles for the O-NO_2 homolysis from NG and subsequent decomposition of the intermediate radicals

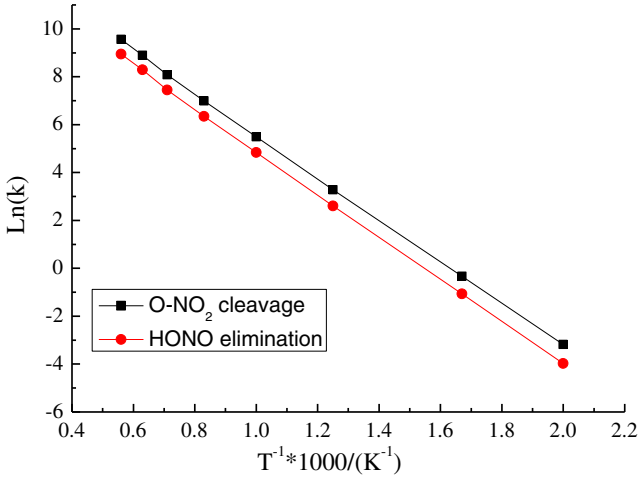

Fig. 5 The rate constants of two initial decomposition channels: O-NO_2 cleavage and HONO elimination

The bond length of β-O-NO_2 in INT2 arrives 2.872 Å, which means that the O-NO_2 bond breaks and the second NO_2 is removed from INT2. Therefore, INT2 decomposes to produce INT3 and NO_2, as shown in Eq. (4). INT3+CH_2O+2NO_2 are 9.19 kJ mol^{-1} more exothermic than NG, indicting that INT3+CH_2O+2NO_2 are more stable than NG.

Similarly, INT3 may further decompose to INT4 via the removal of the third NO_2 group, as shown in Eq. (5). The third NO_2 elimination involves the O-NO_2 breaking, which requires additional energy of 131.12 kJ mol^{-1}. The C-C bond is weaker than other bonds in INT4 and the rupture of the C-C bond is possible. Equation (6) indicates that the C-C bond cleavage in INT4 leads to form CHO and HCHO via TS2, which has a barrier of 148.35 kJ mol^{-1} over NG. The energy barrier for this process at TS2 is 26.42 kJ mol^{-1}. The breaking C-C bond in TS2 is 2.117 Å. The final products of the unimolecular decomposition of NG are •CHO, 2CH_2O, and 3•NO2. They can further react with each other, for example:

$$HCHO + \bullet NO_2 \rightarrow \bullet CHO + HNO_2$$
$$\bullet CHO + \bullet NO_2 \rightarrow CO + HONO$$
$$\bullet CHO + \bullet NO_2 \rightarrow HCOO\bullet + \bullet NO$$
$$HCOO\bullet + \bullet NO_2 \rightarrow CO_2 + HONO$$
$$2HONO \rightarrow H_2O + \bullet NO + \bullet NO_2$$

The small molecules generated here can account for some of the products observed in the experiments [9]. Therefore, our calculated results are supported by the experimental report.

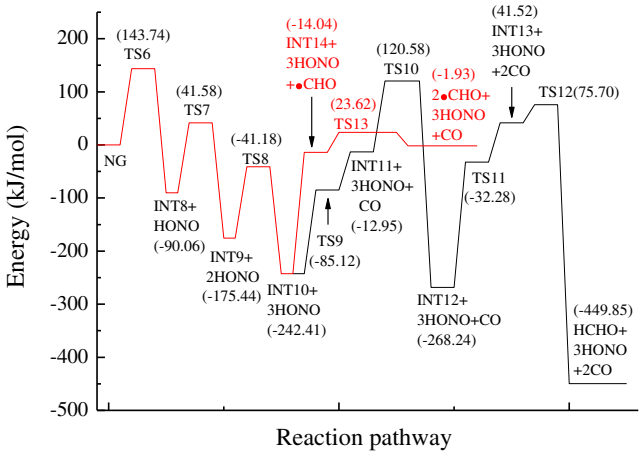

Fig. 4 Potential energy profiles for the HONO elimination from NG and subsequent decomposition of the intermediate radicals

Further cleavage of O-NO_2 in INT1 based on Eqs. (3), (7), (8), (9), and (6)

INT1 is difficult to decompose to form a biradical via the elimination of second NO_2 group. This is because the forming biradical has very high energy and is very unstable, which is similar with the biradical referred to in ref 37. Therefore, the O-NO_2 bond in INT1 can further break to form INT5 via an intramolecular hydrogen transfer, as shown in Eq. (3). For this process we searched and obtained TS3, as shown in Fig. 2. The breaking O-NO_2 bond and C-H bond in TS3 are 1.786 and 1.362 Å, respectively. TS3 has a barrier of 116.74 kJ mol^{-1} over INT1 and decomposes to NO_2 and INT5. In TS3, the O-NO_2 bond length increases and the H atom from its neighboring CH_2 group migrates to the O atom connected with NO_2. This makes its adjacent C-O bond (between the H migrating C and O radical in INT1) present double bond character (1.262 Å). The migrating H atom is 1.392 away from the O atom linked by NO_2 while 1.362 Å away from the C atom. It means that there is a hydrogen transfer in TS3. This is supported by the result that TS3 has a large imaginary frequency of 1863 cm^{-1}, as

Table 1 Calculated frequencies of the intermediates at the B3LYP/6-311G** level[a]

NG								
15	31	37	45	56	63	93	161	170
186	209	245	282	291	448	518	557	578
639	676	702	735	751	765	765	837	858
870	925	928	1028	1046	1106	1110	1143	1254
1287	1302	1323	1327	1338	1408	1414	1425	1502
1510	1755	1757	1778	3051	3059	3104	3108	3122
INT1								
31	38	50	78	110	131	165	225	251
268	333	429	546	562	610	674	725	753
764	773	846	866	923	967	1030	1085	1098
1114	1186	1277	1295	1318	1327	1334	1370	1407
1420	1502	1752	1770	2886	2952	3051	3101	3112
INT2								
18	20	31	53	59	86	102	128	135
216	334	452	630	680	761	767	775	856
1019	1076	1107	1238	1310	1360	1397	1407	1480
1705	1759	1820	2946	3044	3102			
INT3								
37	123	157	200	282	541	634	732	767
785	867	904	1091	1099	1253	1319	1381	1414
1480	1751	1843	2874	3024	3062			
INT4								
162	261	416	701	777	861	1020	1171	1256
1379	1439	1852	2848	2863	2922			
INT5								
50	59	97	127	172	222	287	366	416
477	556	642	700	766	852	867	919	1010
1046	1118	1143	1230	1253	1314	1337	1373	1410
1424	1503	1750	1822	2924	2963	3071	3135	3831
INT6								
44	119	202	288	411	446	487	612	793
835	1008	1030	1072	1106	1160	1233	1271	1332
1358	1374	1421	1811	2867	2907	2967	2997	3774
INT7								
283	425	648	808	820	928	1018	1210	1345
1405	1536	1564	3006	3224	3540			
INT8								
32	43	50	78	91	127	167	220	237
284	362	455	518	583	655	696	704	751
765	833	860	875	926	1024	1076	1094	1135
1261	1278	1317	1329	1369	1395	1417	1504	1755
1781	1825	2932	3045	3073	3132			
INT9								
35	66	81	128	195	286	328	440	489
548	619	652	749	790	843	946	1035	1053
1212	1277	1321	1361	1375	1462	1779	1805	1810
2937	3059	3120						
INT10								
NG								
82	100	171	325	417	530	591	791	949
1031	1224	1361	1373	1787	1799	1832	2915	2922
INT11								
216	256	291	583	925	975	1184	1337	1442
1619	2839	3811						
INT12								
143	333	553	820	1058	1077	1329	1377	1808
1810	2923	2929						
INT13								
458	1076	1157	1301	3045	3671			
INT14								
174	250	679	781	984	1343	1464	2164	2995

[a] ll frequencies are in cm^{-1}

shown in Table 2. INT5+2NO_2 are 75.99 kJ mol^{-1} more exothermic than NG.

INT5 will further decompose to INT6 via the third NO_2 group leaving. The chemical reaction of this process is listed in Eq. (7). The third NO_2 removal involving the breakage of O-NO_2 required an additional 134.01 kJ mol^{-1} energy. It is most likely that the C-C bond (between the O radical C and its neighboring C) will be broken up in INT6 to form INT7 and CH_2O as shown in Eq. (8). The energy barrier for this process at TS4 is 76.64 kJ mol^{-1} over NG. The length of C-C bond in TS4 is 1.923 Å. Equation (9) shows that INT7 can further transform to INT4 by an intramolecular H-transfer. There exists a transition state named TS5, which has a barrier of 224.11 kJ mol^{-1} over NG. In TS5, the H atom from the O-H bond transfers to its adjacent C atom, and the migrating H atom is 1.253 Å and 1.248 Å away from the O and C atoms, respectively. INT4 will also decompose to •CHO and CH_2O via TS2, the same as discussed above. Under this kind of decomposition pathway, we also gain some small unstable products such as •CHO, CH_2O, and •NO_2, which can react with each other as the reaction equation above.

Successive HONO eliminations and subsequent decomposition

First HONO elimination based on Eq. (10)

It is seen from Table 3 that the trigger reaction is the α-H transfer required for a HONO elimination. The α-H transfer and HONO removal take place easily because the α-O-NO_2 bond is weak and the nonbonded CH::O distance is near. This elimination reaction is similar to the HONO elimination in the decomposition of RDX and HMX [36, 37]. TS6 for this process was obtained and has a barrier of 143.74 kJ

Table 2 Calculated frequencies of the transition states at the B3LYP/6-311G** level[a]

TS1								
−329	30	34	42	67	77	107	151	194
219	245	322	366	439	550	582	633	659
706	713	760	797	855	883	950	1005	1122
1132	1162	1236	1266	1312	1334	1381	1420	1451
1497	1595	1752	1816	2884	2939	3074	3137	3183
TS2								
−283	88	166	391	409	718	1057	1129	1238
1474	1615	1954	2765	2825	2850			
TS3								
−1891	35	48	61	79	99	146	160	193
263	279	337	369	398	544	560	587	613
704	758	776	833	862	884	996	1013	1055
1064	1123	1215	1265	1328	1341	1349	1383	1419
1458	1507	1624	1770	1847	2932	3066	3118	3131
TS4								
−514	112	142	210	243	358	390	496	568
724	942	977	1070	1150	1211	1228	1260	1360
1387	1460	1553	1765	2892	2921	2970	3115	3750
TS5								
−1991	194	323	549	556	895	1006	1081	1176
1297	1399	1735	2390	2920	3088			
TS6								
−1532	23	39	50	52	67	90	107	169
175	218	223	256	288	380	400	455	470
547	581	645	660	689	719	763	765	827
852	867	917	968	1017	1064	1079	1137	1220
1255	1282	1304	1311	1327	1345	1382	1406	1467
1503	1598	1751	1754	1805	2951	3067	3089	3128
TS7								
−1487	28	40	82	106	124	145	196	233
245	284	341	431	475	501	547	622	677
708	765	831	858	871	978	1022	1058	1155
1198	1253	1305	1321	1367	1379	1435	1493	1600
1752	1806	1822	2928	3070	3132			
TS8								
−1515	75	77	123	149	204	261	348	405
416	534	548	617	673	788	838	972	1011
1185	1224	1296	1314	1366	1430	1613	1778	1805
1841	2933	2987						
TS9								
−1280	102	158	210	367	471	491	662	684
822	987	1053	1326	1512	1641	1998	2087	2971
TS10								
−2051	157	278	335	579	909	991	1339	1454
1623	2436	2867						
TS11								
−309	82	268	335	645	1162	1879	2060	2825
TS12								
−1271	176	207	611	762	767	1273	1302	1530
1816	2098	2949						
TS13								
−2104	753	1322	1443	2616	2865			

[a] All frequencies are in cm^{-1} and the negative numbers indicate imaginary frequencies

mol^{-1} over NG, slightly higher than the homolysis energy of $O\text{-}NO_2$ discussed above. In TS6, the breaking $O\text{-}NO_2$ and C-H bonds are 2.023 and 1.332 Å, respectively, while the forming O-H, O-N, and C-O bonds are 1.293, 1.241, and 1.283 Å, respectively. The C-O bond near the O radical in INT8 has double bond character (1.200 Å). Besides, the intermediate INT8 and generated HONO is 90.06 kJ mol^{-1} more exothermic than NG, that is to say, this elimination is an exothermic reaction.

Second HONO elimination based on Eq. (11)

On the basis of the first HONO elimination, INT8 further decomposes to INT9 via the second HONO elimination and TS7 is easily found. TS7 for the second HONO elimination has a barrier of 41.58 kJ mol^{-1} over NG, while the relative energy of INT9+2HONO is 175.44 kJ mol^{-1} more exothermic than NG. This shows that the second HONO is easier to eliminate than the first one. As shown in Fig. 2, the lengths of $O\text{-}NO_2$ and C-H bond in TS7 are 1.964 and 1.352 Å, respectively, whereas the lengths of the forming O-H, O-N, and C-O bonds are 1.280 Å, 1.243 Å, and 1.294 Å, respectively.

Third HONO elimination based on Eq. (12)

INT9 can subsequently eliminate the third HONO to form an intermediate INT10 via TS8, which has the energy of

Table 3 Relative energies for two competitive initial decompositions of NG at the B3LYP/6-311G**and B3LYP/6-311++G** level

	Relative energy (kJ mol^{-1})
$O\text{-}NO_2$ bond cleavage	
The bond dissociation energy (BDE) of α-$O\text{-}NO_2$	133.34(125.43)
The bond dissociation energy of β-$O\text{-}NO_2$	138.78(131.08)
HONO elimination	
α-H transfer TS	143.74(143.63)
β-H transfer TS	156.72(155.19)

The values in parentheses is calculated at B3LYP/6-311++G** level

41.18 kJ mol^{-1} below NG. INT10+3HONO are 242.41 kJ mol^{-1} more exothermic than NG. In TS8, the breaking O-NO_2 and C-H bond and the forming O-H, O-N, and C-O bond are 1.958 Å, 1.367 Å, 1.256 Å, 1.246 Å, and 1.291 Å, respectively. Thus, it may be concluded from the discussion above that the HONO elimination from NG is the most exothermic pathway found in the present study.

INT10 decomposition plus subsequent decomposition based on Eqs. (13), (14), (15), (16), (17), and (18)

Equations (13) and (14) show that there are two possible pathways for the decomposition of INT10: one is the H-transfer reaction and the other is the rupture of the C-C bond. INT10 with three carbonyl groups, named oxopropanedial, is unstable. It can further decompose to INT11 and a stable CO via a hydrogen transfer and simultaneous C-C bond rupture, as shown in Eq. (13). The energy barrier for this process at TS9 is 157.29 kJ mol^{-1} with respect to INT10. As the length of C-C bond increases in TS9, the H atom from the first C atom migrates to the O atom from the third C atom. In TS9, the C-C bond distance is 2.010 Å and the migrating H atom is 1.273 Å and 1.350 Å away from the C and O atoms, respectively. INT11 is active and can transform to INT12 via another H transfer (the H atom from the O atom migrating to its adjacent C atom). The chemical reaction for this process is listed in Eq. (15). TS10 for this process was obtained and has a barrier of 120.58 kJ mol^{-1} over NG. The migrating H atom is 1.208 Å away from the O atom while 1.279 Å away from the C atom. Similarly, it is seen from Eq. (12) that INT12, named glyoxal, can further decompose to INT13 and a stable CO molecule via TS11. The mechanism of this reaction is similar to the decomposition of INT10. TS11 has an energy barrier of 32.28 kJ mol^{-1} below NG. In TS11, the breaking C-C bond is 2.122 Å and the migrating H atom is 1.421 and 1.221 Å away from the C and O atoms, respectively. As shown in Fig. 4, INT13 is unstable and can quickly transform to CH_2O via TS12, which has a barrier of 34.18 kJ mol^{-1} over INT13. The chemical reaction for this process is listed in Eq. (17). The final products are CH_2O+3HONO+2CO, which is 449.85 kJ mol^{-1} more exothermic than NG.

Equation (14) shows that another decomposition pathway of INT10 is the C-C cleavage and the bond dissociation energy of the C-C bond is 228.37 kJ mol^{-1}. The decomposition products are INT14 and •CHO. INT14 can further decompose to CO and •CHO via TS13 (another C-C bond rupture), as shown in Eq. (18). The energy barrier for this process at TS13 is 37.66 kJ mol^{-1} over INT14. In TS13, the breaking C-C bond is 2.024 Å. The final products are 2•CHO+3HONO+CO, which are 1.93 kJ mol^{-1} more exothermic than NG.

Rate constants of initial decomposition process

There are two main mechanisms for the unimolecular decomposition of NG and the detailed mechanism has discussed above. The energies and the molecular parameters obtained from the ab initio calculations can be applied in the rate constant calculation. Here, we only calculated the rate constants of the initial decomposition process of NG.

The transition state theory of Eyring was used to calculate the rate constants as the following equation:

$$k = \frac{k_B T}{h}\left(\frac{p^o}{RT}\right)^{1-n} \exp\left[\frac{\Delta_r^{\neq} S_m^o(p^o)}{R}\right] \exp\left[-\frac{\Delta_r^{\neq} H_m^o(p^o)}{RT}\right], \quad (19)$$

where k_B is Boltzmann constant, h is Plank constant, $\Delta_r^{\neq} S_m^o(p^o)$ and $\Delta_r^{\neq} H_m^o(p^o)$ are standard molar entropy and standard molar enthalpy of activation at the condition of $p^o = 100$ kPa, respectively, and n is the sum of computation coefficient for all reactants. For the initial decomposition reaction here, n=1.

As seen in Fig. 5, the rate constants of the HONO elimination increase slightly faster than those of the O-NO_2 cleavage reaction with increasing temperature. However, there is no crossover among the two lines, that is to say, the rate constant of O-NO_2 cleavage reaction is higher than that of HONO elimination over the temperature range of 500–1800 K. Under 530 K, the rate constants of the two initial reactions are less than 0.1 s^{-1}. This indicates that the two reactions take place by low reaction rates. When the temperature is over 700 K, the two initial reactions occur rapidly. The linear relationship between ln(k) and 1/T for the O-NO_2 cleavage reaction is ln(k)=14.375–8815.2/T, while for the HONO elimination reaction the linear relationship is ln(k)=13.841–8943.6/T. Therefore, it can be concluded that the O-NO_2 cleavage in the initial decomposition of NG occurs more easily than the HONO elimination, which is consistent with the discussion above.

Conclusions

In this work, we have studied detailed mechanisms for the unimolecular decomposition of NG in gas phase at the DFT-B3LYP/6-311G** level. The consecutive HONO elimination to form INT10 and 3HONO is identified as the energetically favorable decomposition pathway. INT10 can further decompose to CH_2O+2CO and 2•CHO+CO. Besides, the O-NO_2 bond homolysis to form INT1 is also favorable, but the associated endothermicity for subsequent decomposition makes this pathway less favorable than the other. INT1 can further decompose to •CHO+2CH_2O. The small molecules generated can account for some of the

products observed in the experiments. The HONO elimination decomposition channel is exothermic, while the O-NO_2 cleavage reaction is endothermic. An analysis of the rate constants for the two initial decompositions shows that the O-NO_2 cleavage reaction occurs more easily than the HONO elimination.

Acknowledgments This work was supported by the National "973" Project.

References

1. Sadasivan N, Bhaumik A (1984) J Therm Anal 29:1043–1052
2. Li SN, Liu Y, Tuo XL, Wang XG (2008) Polymer 49:2775–2780
3. McDonald BA (2011) Propell Explos Pyrot 36:576–583
4. Yi JH, Zhao FQ, Xu SY, Gao HX, Hu RZ (2008) Chem Res Chinese U 24:608–614
5. Sui X, Wang NF, Wan QA, Bi SH (2010) Propell Explos Pyrot 35:535–539
6. Zhao YJ, Zhang W, Zhang XG, Zhu H, Wang CH, Fang LJ (2007) Theory Pract Energ Mater 7:163–166
7. Zhang TH (2002) J Energ Mater 20:175–189
8. Hiegel GA, Nguyen J, Zhou Y (2004) Synth Commun 34:2507–2511
9. Chas EW, Krastins G (1970) J Phys Chem 74:999–1006
10. Roos BD, Brill TB (2002) Combust Flame 128:181–190
11. Hiyoshi RI, Brill TB (2002) Propell Explos Pyrot 27:23–30
12. Chin A, Ellison DS, Poehlein SK (2007) Propell Explos Pyrot 32:117–126
13. Roos BD, Brill TB (2001) Propell Explos Pyrot 26:213–220
14. Tompa AS (1980) J Hazard Mater 4:95–112
15. Sućeska M, Mušanić SM, Houra IF (2010) Thermochim Acta 510:9–16
16. Toland A, Simmie JM (2003) Combust Flame 132:556–564
17. Devyatykh GG, Zaslonko IS, Smirnov VN, Moiseev AN, Votintsev VN, Tereza AM (1993) Kinet Catal 34:185–189
18. Oxley JC, Smith JL, Rogers E, Ye W, Aradi AA, Henly TJ (2000) Energ Fuel 14:1252–1264
19. Correra TC, Riveros JM (2010) J Phys Chem A 114:11910–11919
20. Makashir PS, Mahajan RR, Agrawal JP (1995) J Therm Anal 45:501–509
21. Michael AH, Kay RB, Jimmie CO (1991) J Phys Chem 95:3955–3960
22. Francisco MA, Krylowski J (2005) Ind Eng Chem Res 44:5439–5446
23. Gong XD, Xiao HM (2000) J Mol Struc (Theochem) 498:181–190
24. Gong XD, Xiao HM (2001) J Mol Struc (Theochem) 572:213–221
25. Wang DX, Xiao HM (1992) J Phys Org Chem 5:361–366
26. Tan JZ, Xiao HM, Gong XD, Li JS (2001) Chinese J Chem 19:931–937
27. Li MM, Wang GX, Guo XD, Wu ZW, Song HC (2009) J Mol Struc (Theochem) 900:90–95
28. Yonei T, Hashimoto K, Arai M, Tamura M (2003) Energ Fuel 17:725–730
29. Xiao HM, Fan JF, Li YF (1990) Chinese J Chem 8:390–395
30. Becke AD (1993) J Chem Phys 98:5648–5652
31. Lee C, Yang W, Parr RG (1988) Phys Rev B 37:785–789
32. Gonzalez C, Schlegel HB (1989) J Chem Phys 90:2154
33. Gonzalez C, Schlegel HB (1990) J Phys Chem 94:5523
34. Frisch MJ, Trucks GW, Schlegel HB, Scuseria GE, Robb MA, Cheeseman JR, Montgomery JA Jr, Vreven T, Kudin KN, Burant JC, Millam JM, Iyengar SS, Tomasi J, Barone V, Mennucci B, Cossi M, Scalmani G, Rega N, Petersson GA, Nakatsuji H, Hada M, Ehara M, Toyota K, Fukuda R, Hasegawa J, Ishida M, Nakajima T, Honda Y, Kitao O, Nakai H, Klene M, Li X, Knox JE, Hratchian HP, Cross JB, Adamo C, Jaramillo J, Gomperts R, Stratmann RE, Yazyev O, Austin AJ, Cammi R, Pomelli C, Ochterski JW, Ayala PY, Morokuma K, Voth GA, Salvador P, Dannenberg JJ, Zakrzewski VG, Dapprich S, Daniels AD, Strain MC, Farkas O, Malick DK, Rabuck AD, Raghavachari K, Foresman JB, Ortiz JV, Cui Q, Baboul AG, Clifford S, Cioslowski J, Stefanov BB, Liu G, Liashenko A, Piskorz P, Komaromi I, Martin RL, Fox DJ, Keith T, Al-Laham MA, Peng CY, Nanayakkara A, Challacombe M, Gill PMW, Johnson B, Chen W, Wong MW, Gonzalez C, Pople JA (2003) Gaussian 03. Gaussian, Inc., Pittsburgh, PA
35. Luo YR (2003) Handbook of bond dissociation energies in organic compouds. CRC Press, Washington, DC
36. Chakraborty D, Muller RP, Dasgupta S, Goddard WA (2001) J Phys Chem A 105:1302–1314
37. Chakraborty D, Muller RP, Dasgupta S, Goddard WA (2000) J Phys Chem A 104:2261–2272